

MICROBUNCHING GAIN OF THE WISCONSIN FEL BEAM SPREADER*

R. A. Bosch[#] and K. J. Kleman, Synchrotron Radiation Center, University of Wisconsin-Madison,
3731 Schneider Dr., Stoughton, WI 53589, U.S.A.

J. Wu, Stanford Linear Accelerator Center, Stanford University, Stanford, CA 94309 U.S.A.

Abstract

The microbunching gain of a free-electron laser (FEL) driver is affected by the beam spreader that distributes bunches to the FEL beam lines. For the Wisconsin FEL (WiFEL), analytic formulas and tracking simulations indicate that a beam spreader design with a low value of R_{56} has little effect upon the gain.

INTRODUCTION

A preliminary design of the WiFEL driver utilizes a two-stage compression and acceleration system to transform a 4-MeV bunch with peak current of 50 A into a 1.7-GeV bunch with peak current of 1 kA [1]. The compressed bunch is distributed to an FEL beam line and collimated by passing through a three-stage beam spreader [1]. To prevent large current or energy modulations at the FEL, the microbunching gain contribution of the beam spreader should be small.

For WiFEL, analytic estimates and simulations indicate that a spreader design whose R_{56} matrix element is 1 mm contributes significant microbunching gain, while a design whose R_{56} value is $\ll 1$ mm contributes little gain. This is consistent with studies of the FERMI linac, where a small gain contribution was obtained when the R_{56} value of the spreader was $\ll 1$ mm [2].

MULTI-STAGE GAIN

When a bunch's longitudinal distribution is frozen between chicanes, the linear microbunching gain of a multi-stage compression and acceleration system may be approximated by modeling staged compression [3]. A frozen chirped bunch with energy E_{in} and peak current magnitude I_0 is accelerated to energy E_1 while passing through impedance Z_{zero} . It is compressed by a factor C_1 by the energy-to-position matrix element $R_{56}^{(1)}$ of the BC1 chicane, and accelerated to energy E_2 while passing through impedance Z_1 . It is then compressed by a factor C_2 by the $R_{56}^{(2)}$ of the BC2 chicane, and accelerated to the energy E_3 while passing through impedance Z_2 . In the n -th stage, the chirped bunch is compressed by a factor C_n by the matrix element $R_{56}^{(n)}$, and accelerated to the energy E_{n+1} while passing through impedance Z_n .

When $E_{in} = E_1$ and the impedance Z_{zero} is zero, the microbunching growth of a current or energy modulation

with initial wavenumber k_0 on a bunch entering BC1 with energy E_1 is described by a matrix

$$T \equiv \begin{pmatrix} T_{II} & T_{IE} \\ T_{EI} & T_{EE} \end{pmatrix}, \quad (1)$$

in which the growth of the current and energy modulations obey $T_{II} = (\Delta I / I_{out}) / (\Delta I / I_{in})$, $T_{IE} = (\Delta I / I_{out}) / (\Delta E / E_{in})$, $T_{EI} = (\Delta E / E_{out}) / (\Delta I / I_{in})$ and $T_{EE} = (\Delta E / E_{out}) / (\Delta E / E_{in})$.

For single-stage compression followed by acceleration to the energy $E_{out} = E_2$, we have [3]

$$T_{II} = F_1, \quad (2a)$$

$$T_{IE} = iF_1 C_1 k_0 R_{56}^{(1)}, \quad (2b)$$

$$T_{EI} = \frac{-F_1 C_1 e Z_1 I_0}{E_{out}} + \frac{iG_1 C_1}{E_{out}}, \quad (2c)$$

$$T_{EE} = \frac{F_1 C_1 E_1}{E_{out}} - \frac{G_1 C_1^2 k_0 R_{56}^{(1)}}{E_{out}} - \frac{iF_1 C_1^2 e Z_1 I_0 k_0 R_{56}^{(1)}}{E_{out}}, \quad (2d)$$

where the reduction in growth at short wavelengths from the bunch's energy spread is described by the quantities

$$F_1 = \int \cos(k_0 C_1 R_{56}^{(1)} \delta / E_1) f(\delta) d\delta, \quad (3)$$

$$G_1 = \int \delta \sin(k_0 C_1 R_{56}^{(1)} \delta / E_1) f(\delta) d\delta$$

Here, $e > 0$ is the magnitude of the electron charge, $f(\delta)$ is the normalized energy distribution of each slice of the uncompressed bunch, and the impedance Z_1 is evaluated at the compressed wavenumber $C_1 k_0$.

For two-stage compression, the matrix T may be obtained by modeling the rotated phase space entering the second chicane [3]. For more than two stages, the expressions become intractable. However, if we neglect the phase-space rotation at the entrance of the n -th stage for $n > 1$, the multistage gain may be approximated by matrix multiplication of the single-stage gain matrix, as in the case of a cold bunch, so that $T \approx T^{(n)} T^{(n-1)} \dots T^{(1)}$. The gain matrix $T^{(n)}$ for the n -th stage is given by eqs. (1)–(3), in which the compression factor, R_{56} -value, impedance and energies describe the n -th stage, while the wavenumber, peak current and energy distribution describe the bunch at the entrance of the n -th stage. This gives the elements of $T^{(n)}$

$$T_{II}^{(n)} = F^{(n)}, \quad (4a)$$

$$T_{IE}^{(n)} = iF^{(n)} k_0 R_{56}^{(n)} (\prod_{j=1}^n C_j), \quad (4b)$$

*Work supported by NSF grant DMR-0537588

[#]bosch@src.wisc.edu

$$T_{EI}^{(n)} = \frac{-F^{(n)}eZ_n I_0 (\prod_{j=1}^n C_j)}{E_{n+1}} + \frac{iG^{(n)}C_n}{E_{n+1}}, \quad (4c)$$

$$T_{EE}^{(n)} = \frac{F^{(n)}C_n E_n}{E_{n+1}} - \frac{G^{(n)}k_0 R_{56}^{(n)}C_n (\prod_{j=1}^n C_j)}{E_{n+1}} - \frac{iF^{(n)}eZ_n I_0 k_0 R_{56}^{(n)} (\prod_{j=1}^n C_j)^2}{E_{n+1}}, \quad (4d)$$

where

$$F^{(n)} = \int \cos[(\prod_{j=1}^{n-1} C_j)^2 C_n k_0 R_{56}^{(n)} \delta / E_n] f(\delta) d\delta, \quad (5)$$

$$G^{(n)} = (\prod_{j=1}^{n-1} C_j) \int \delta \sin[(\prod_{j=1}^{n-1} C_j)^2 C_n k_0 R_{56}^{(n)} \delta / E_n] f(\delta) d\delta.$$

Here, $f(\delta)$ is the energy distribution of each slice of the uncompressed bunch. The impedance Z_n is evaluated at compressed wavenumber $(\prod_{j=1}^n C_n)k_0$. Note that $F^{(3)}$, $G^{(2)}$ and $G^{(3)}$ differ from F_3 , G_2 and G_3 in Ref. [3].

For a bunch with initial energy $E_{in} \leq E_1$ that experiences impedance Z_{zero} before compression, the gain is [3]

$$\frac{\Delta I / I_{out}}{\Delta I / I_{in}} = T_{II} - \frac{eZ_{zero}(k_0)I_0}{E_1} T_{IE} \quad (6a)$$

$$\frac{\Delta E / E_{out}}{\Delta I / I_{in}} = T_{EI} - \frac{eZ_{zero}(k_0)I_0}{E_1} T_{EE} \quad (6b)$$

$$\frac{\Delta I / I_{out}}{\Delta E / E_{in}} = \frac{E_{in}}{E_1} T_{IE} \quad (6c)$$

$$\frac{\Delta E / E_{out}}{\Delta E / E_{in}} = \frac{E_{in}}{E_1} T_{EE}. \quad (6d)$$

Note that eq. (6) may be obtained by multiplying $T \approx T^{(n)} T^{(n-1)} \dots T^{(1)}$ on the right with matrix $T^{(0)}$ that describes a stage with $R_{56}^{(0)} = 0$, compression $C_0 = 1$, and impedance Z_{zero} .

For the WIFEL preliminary two-stage compressor (without a beam spreader), we compared the gain given by the approximation $T \approx T^{(2)} T^{(1)}$ with the matrix T obtained by modeling the rotated phase space entering the second chicane [3]. For realistic initial energy spreads of 1–10 keV rms, the gain for Gaussian energy distributions was accurately given by the approximation $T \approx T^{(2)} T^{(1)}$. For the energy distribution produced by a matched laserheater, good agreement was obtained. We have previously found that the gain matrix T agrees with simulations performed with the code ELEGANT [3, 4].

BEAM SPREADER

The WIFEL beam spreader separates the compressed bunches for different FELs in three stages, where each stage has RF separation amplified by a defocusing quadrupole magnet, followed by dipole bending magnets [1], and then collimates the beam to decrease its halo. To estimate the microbunching gain through the spreader, we

model each of the spreader stages and the collimator as a compression stage with nonzero R_{56} followed by impedance. Since the bunch chirp is nearly zero in the spreader, each stage has compression factor of one.

To model the impedance in the spreaders and collimator for wavelengths shorter than the bunch length, we use the one-dimensional (1D) model of the longitudinal space charge (LSC) impedance, approximated as the impedance of a round beam with effective radius $r_b = 0.85(\sigma_x + \sigma_y)$ [3, 5, 6]. The beam dimensions are those of a bunch with normalized transverse emittances of 1 μm -rad in a magnet lattice whose beta functions obey $\langle \beta_x \rangle \approx \langle \beta_y \rangle \approx 25 \text{ m}$. We expect this 1D model to apply when the beam diameter $2r_b$ is smaller than the radial extent of an electron's relativistically contracted Coulomb field $\lambda\gamma/2\pi$, i.e. $\lambda \geq 4\pi r_b / \gamma$, where λ is the wavelength and γ is the relativistic factor in the spreader [6]. This applies to initial wavelengths λ_0 that exceed 0.01 mm.

In our first spreader design, the R_{56} values of the spreader stages (S1, S2 and S3) and collimator (CO), in the convention where a chicane has negative R_{56} , are $R_{56}^{(S1)} = 182 \mu\text{m}$, $R_{56}^{(S2)} = 750 \mu\text{m}$, $R_{56}^{(S3)} = -105 \mu\text{m}$ and $R_{56}^{(CO)} = 123 \mu\text{m}$. The R_{56} value of the entire spreader, given by summing the R_{56} of each stage and the collimator, is 950 μm . The lengths over which the LSC impedance acts are $L_{S1} = 74.76 \text{ m}$, $L_{S2} = 37.40 \text{ m}$, $L_{S3} = 44.40 \text{ m}$ and $L_{CO} = 71.77 \text{ m}$.

For a chirped bunch entering the BC1 chicane with current of 50 A, normalized transverse emittances of 1 μm , energy of 215 MeV and 3-keV Gaussian energy spread, the solid curves in Fig. 1(a) show the analytic microbunching gain through the exit of the spreader tree at 1.7 GeV, as a function of the modulation's initial wavelength. The gain for two stages of compression followed by three spreader stages and one stage of collimation is approximated by matrix multiplication. Dashed curves show the analytic microbunching gain through the entrance of the spreader tree. The analytic model includes linac geometric wakes, coherent radiation in magnets and drift regions, and LSC in the linac and all drift regions [3]. (Note that LSC in drift regions was omitted in Ref. [3].)

We plot circles to show the gain in ELEGANT tracking simulations of 4 million particles in a 200-pC modulated bunch whose initial parabolic profile has rms length of 0.4 mm and peak current of 50 A, using rf parameters that are adjusted to compensate the macroscopic effects of wakes [3]. The simulations, which utilize noise-reduction techniques described in Ref. [3], include a 1D model of LSC, a 1D model of coherent radiation in magnets and drift regions, in addition to geometric wakes of the linacs and resistive-wall wakes for the spreader's vacuum

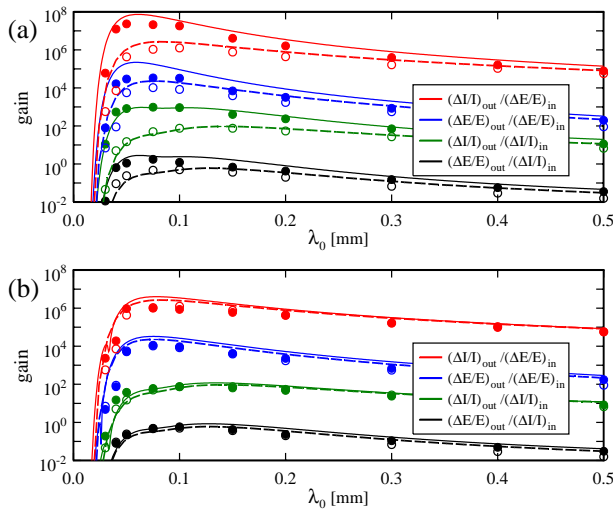


Figure 1: Solid curves show the analytic microbunching gain between the entrance of the BC1 chicane and the exit of the spreader tree versus initial wavelength λ_0 . Dashed curves show the analytic gain between the entrance of BC1 and the entrance of the spreader tree. Filled circles show the gain from the entrance of BC1 through the exit of the spreader tree from tracking simulations, while open circles show the simulated gain between the entrance of BC1 and the entrance of the spreader tree. (a) First spreader design. (b) Low- R_{56} design.

chambers. The simulations and analytic estimates are in good agreement. The spreader increases the peak microbunching gain by more than an order of magnitude.

To reduce the microbunching gain, we created a new spreader design in which the R_{56} value of the entire spreader is reduced by 96% to $38.5 \mu\text{m}$. In this low- R_{56} design, $R_{56}^{(S1)} = 16 \mu\text{m}$, $R_{56}^{(S2)} = 8.5 \mu\text{m}$, $R_{56}^{(S3)} = -109 \mu\text{m}$ and $R_{56}^{(CO)} = 123 \mu\text{m}$. The lengths are $L_{S1} = 72 \text{ m}$, $L_{S2} = 40.05 \text{ m}$, $L_{S3} = 45.10 \text{ m}$ and $L_{CO} = 71.77 \text{ m}$.

Figure 1(b) shows that the analytic gain curves at the entrance and exit of the low- R_{56} spreader are nearly the same, in agreement with ELEGANT simulations.

SHOT NOISE

Let us estimate the modulations at the spreader exit from amplified shot noise, for a 200-pC parabolic bunch with normalized transverse emittances of $1 \mu\text{m}$, 3-keV Gaussian energy spread and peak current of 50 A. For each initial wavelength, we assume the initial rms shot noise obeys $\Delta I / I_{\text{in}} = 1 / \sqrt{N_b}$ [6], where $N_b = 1.25 \times 10^9$ is the number of electrons in the bunch. We calculate the energy modulation at the entrance of the BC1 chicane for a current modulation $\Delta I / I_{\text{in}}$ that is frozen while the bunch is accelerated at a constant rate from 4 MeV to 215 MeV in the injector linac of length 43.6 m, while

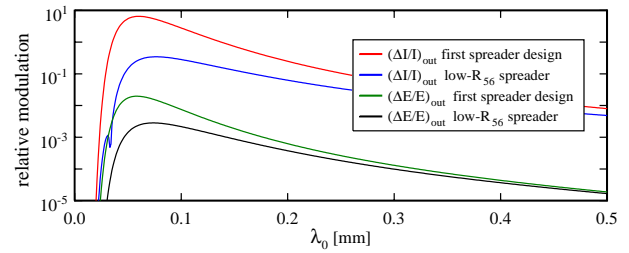


Figure 2: Relative current and energy modulations at the exit of the spreader tree from linear amplification of shot noise, versus initial wavelength λ_0 . Analytic calculations are shown for both spreader designs.

experiencing the 1D LSC impedance evaluated for $\langle \beta_x \rangle \approx \langle \beta_y \rangle \approx 25 \text{ m}$. Using the analytic gain curves of Fig. 1, we calculate the linear amplification of the current and energy modulations entering BC1. Figure 2 shows the rms current and energy modulations at the spreader exit. For both spreaders, the relative current and energy modulations for $\lambda_0 \sim 50 \mu\text{m}$ exceed the allowed values of 10% and 3×10^{-4} [3]. This suggests that a laser heater will be required to reduce the amplified noise of the two-stage compression and acceleration system [3, 5].

SUMMARY

For WiFEL, a 3-stage beam spreader distributes the compressed bunches to the FEL beam lines. Using analytic estimates and simulations, we have studied the contribution of the beam spreader to the microbunching gain of a two-stage compression and acceleration system. The first spreader design, whose R_{56} value is $950 \mu\text{m}$, increases the peak microbunching gain by more than an order of magnitude. With a new design whose R_{56} value is reduced to $38.5 \mu\text{m}$, the beam spreader has little effect upon the microbunching gain.

REFERENCES

- [1] J. J. Bisognano, R. A. Bosch, M. A. Green, K. D. Jacobs, K. J. Kleman, R. A. Legg, J. Chen, W. S. Graves, F. X. Kärtner and J. Kim, in *Proceedings of the 2007 Particle Accelerator Conference, Albuquerque, NM* (IEEE, Piscataway, NJ, 2007), p. 1281.
- [2] M. Venturini and A. Zholents, Nucl. Instrum. Methods Phys. Res., Sect. A **593**, 53 (2008).
- [3] R. A. Bosch, K. J. Kleman and J. Wu, Phys. Rev. ST Accel. Beams **11**, 090702 (2008).
- [4] M. Borland, Advanced Photon Source Light Source Note LS-287, 2000.
- [5] Z. Huang, M. Borland, P. Emma, J. Wu, C. Limborg, G. Stupakov and J. Welch, Phys. Rev. ST Accel. Beams **7**, 074401 (2004).
- [6] M. Venturini, Phys. Rev. ST Accel. Beams **11**, 034401 (2008).